Vol. 39, No. 2 (2017) 270-276, DOI: 10.24874/ti.2017.39.02.15

Tribology in Industry

www.tribology.fink.rs

RESEARCH

Electroless Ni–B Coating of Pure Titanium Surface for Enhanced Tribocorrosion Performance in Artificial Saliva and Antibacterial Activity

F. Mindivan[a,d], H. Mindivan[b,d], C. Darcan[c,d]

[a]*Bilecik Seyh Edebali University, Bozuyuk Vocational College, Department of Technical Programs, Bilecik, Turkey.*
[b]*Bilecik Seyh Edebali University, Engineering Faculty, Department of Mechanical Engineering, Bilecik, Turkey.*
[c]*Bilecik Seyh Edebali University, Faculty of Arts and Science, Department of Molecular Biology and Genetics, Bilecik, Turkey.*
[d]*Bilecik Seyh Edebali University, Biotechnology Application and Research Center, Bilecik, Turkey.*

Keywords:

Antibacterial
Electroless Ni-B coating
Ttitanium alloy
Triborocorrosion

Corresponding author:

Harun Mindivan
Bilecik Seyh Edebali University,
Engineering Faculty,
Department of Mechanical Engineering,
Bilecik, Turkey.
E-mail: harun.mindivan@bilecik.edu.tr

A B S T R A C T

In the present study, the surface of commercial pure (Grade 2) titanium was coated with electroless Ni–B. The surface morphology, microstructure and phase identification were analysed by X-Ray Diffraction (XRD) and Field Emission Gun Scanning Electron Microscope (FEG-SEM) equipped with Energy Dispersive X-ray Spectroscopy (EDS). The tribocorrosion performance in a laboratory simulated artificial saliva was investigated using a reciprocating ball-on-plate tribometer coupled to an electrochemical cell. The antibacterial property of the electroless Ni–B film coated on pure titanium was basically investigated. From this study, it may be concluded that this electroless Ni–B coating process cannot only improve the hardness and tribocorrosion performance of the pure titanium, but can also provide antimicrobial activity.

1. INTRODUCTION

Titanium (Ti) and its alloys have become one of the most attractive biomaterials thanks to their remarkable mechanical and corrosion resistance properties, as well as biocompatibility. However, the formation of a bacterial surface biofilm, compromised immunity at the implant/tissue interface and poor tribological performance may lead to persistent infections on and around corrosion resistant Ti biomaterials used in corrosive environments [1,2]. Thus, numerous strategies focusing on the surface modification of Ti alloys have been employed to render them protection from both wear, corrosion and even tribocorrosion [3-5]. The strategies include physical vapour deposition [6], thermal spray [6,7], ion or laser nitriding [8-10], thermal oxidation [11,12], micro-arc oxidation [13-15], diffusion [16] and anodic oxidation treatments [17]. On the other hand, the antibacterial properties are also necessary for Ti implant

when exposed to the living tissue [18]. To add biofunction to Ti alloys, a process that changes a material's surface composition, structure, and morphology, leaving the bulk mechanical properties intact is necessary.

Antimicrobial, hard, wear and corrosion resistant surfaces reduce infection complications to prolong the useful life of dental and orthopedic implant materials. By doing so, surface engineered Ti implants could be able to withstand corrosive environment while simultaneously offering an improved wear protection and antibacterial activity. To achieve the desired results, electroless Ni-B coatings are good candidates to use in a variety of industrial applications for the following reasons: their unique properties, such as high hardness, low wear, lubricity, uniform thickness, good ductility, excellent solderability and antibacterial activity [19]. The aim of the present study is to investigate the effect of electroless Ni–B coating on the structural, tribocorrosion and antibacterial properties of commercial pure Ti (CP-Ti), which has not been reported yet.

2. EXPERIMENTAL METHODS

The CP-Ti (Grade 2) having a dimension of 20×20×1 mm3 was used as the substrate material. Before deposition, the surface of the CP-Ti samples was degreased with acetone, and rinsed with distilled water, and picked in 6 % HF for ≅1 min at room temperature and then washed thoroughly with distilled water and dried in air. The chemical composition and operation conditions of the electroless Ni-B solution are reported in Table 1.

Table 1. Bath composition and operation conditions.

Composition	**Ni-B**
Nickel chloride	20 g L^{-1}
Sodium hydroxide	90 g L^{-1}
Sodium borohydride	1 g L^{-1}
Tallium nitrate	0.11 g L^{-1}
Ethylendiamine	100 ml L^{-1}
Bath temperature	90 °C
pH of solution	> 12

The surface and cross-section morphologies of the Ni-B coated CP-Ti were examined by Field Emission Gun Scanning Electron Microscope (FEG-SEM) equipped with Energy Dispersive X-ray Spectroscopy (EDS) and Nikon Eclipse LV150 Light Optic Microscope (LOM), respectively. The phase constituents of the untreated CP-Ti and the Ni-B coated CP-Ti were determined by X-ray diffraction (XRD) using CuK_{α} radiation with a Panalytical Empyrean diffractometer. The cross-sectional hardness measurement was accomplished using Knoop diamond indentation under a 10 g load for a period of 15 seconds. The obtained results were the average of five measurements.

Tribocorrosion experiments were conducted in a triboelectrochemical cell containing 25 ml of simulated artificial saliva (SAS) installed on a linear reciprocating ball-on-flat tribometer with the working surface of the testing samples facing upwards against the counter material (10 mm diameter Al_2O_3 ball). Reciprocating sliding tests were carried out under Open Circuit Potential (OCP) conditions. OCP was monitored before, during and after reciprocation sliding contact with the Al_2O_3 ball. A potentiostat was used to record the potential between the testing sample and the reference electrode during tribocorrosion tests. The tribocorrosion tests consisted of the three steps: (1) stabilization of the system under the OCP for 600 s (in absence of sliding) to achieve a stable passive surface; (2) sliding under the OCP for 2700 s; (3) re-stabilization of the system under OCP (after sliding was stopped) for 600 s. The sliding started in a reciprocating system with total stroke length of 10 mm, sliding speed of 1.7 cm s^{-1}, normal load of 5 N and total sliding distance of 50 m. During the test, sample surface with an area of 1.5 cm^2 was exposed to the corrosive electrolyte. After tribocorrosion tests, the wear scars and Al_2O_3 balls were cleaned following the same cleaning procedure applied before testing and the contact surfaces of wear scars and Al2O3 balls were examined by SEM and LOM, respectively. Total material loss rates were determined by measuring the 2-D cross-sectional area profile of the wear scars (in three locations) by using a contact profilometer (Mitutoyo Surtest SJ-400) and converting this to a wear volume by taking account of the scar length. By the end of the OCP tribocorrosion tests, optical densities of SAS solution were measured using a UV-Spectrophotometer. Freshly prepared SAS was analysed as the reference to evaluate the optical densities of solutions. After the spectrophotometric

measurement of freshly prepared SAS solution by using fix visible light (wave length: 250 nm), the data obtained was automatically adjusted to zero in order to determine the optical densities of the SAS solutions utilized in the OCP tribocorrosion tests.

The antibacterial activity of electroless Ni–B coating on a CP-Ti substrate was determined using Escherichia coli O157:H7 (E. coli, Gram negative) by a disc diffusion method on nutrient agar medium. The untreated CP-Ti was used as a control. Bacterial suspensions (10^8 colony forming units/mL final cell concentrations) were poured into Petri dishes (9 cm) from flasks containing 25 mL sterile nutrient agar. Then the bacteria were evenly distributed over agar surface by a sterile bent. In this way, the large part of the bacteria was on the growth medium for cultivation. The inoculated plates were incubated aerobically at 37 ⍰C for E. coli for 24 h, and then testing results were assessed. By measuring the diameter of the circular shape around the samples, which is inhibition halo (technically known as a ‘‘plaque’’, or zone of inhibition), provided information about the sensitivity or resistance of the cultivated microorganism to the biocide coating. All of the tests were done in triplicates.

3. RESULTS AND DISCUSSION

Figures 1a and 1b displays the morphological and cross-sectional micrographs of the deposited electroless Ni–B coating on the CP-Ti substrate, respectively. The result of Figs. 1a and 1b signs a columnar morphology without porosity and cracks, with a typical cauliflower-like surface texture. In fact this kind of surface morphology is responsible for the lubricious characteristics of the Ni-B coatings [19,20]. It is evident that a deposit close to 15 μm is achieved at the CP-Ti substrate surface and the nickel agglomerates are distributed randomly in it. As is obvious in this figure, a desirable adhesion was established between the Ni-B coating and CP-Ti substrate.

Figure 2 shows the EDS spectra of the Ni-B coated CP-Ti. Quantitative elemental analysis of the coating indicates that the amount of boron is between 4 to 7 wt.%. Some researchers [21] have noted that boron content of electroless Ni–B coatings ranges almost from 1 to 10 wt.%, and the electroless Ni–B coating is amorphous for boron content higher than 5 wt.% [22,23], as suggested by XRD data (Fig. 3).

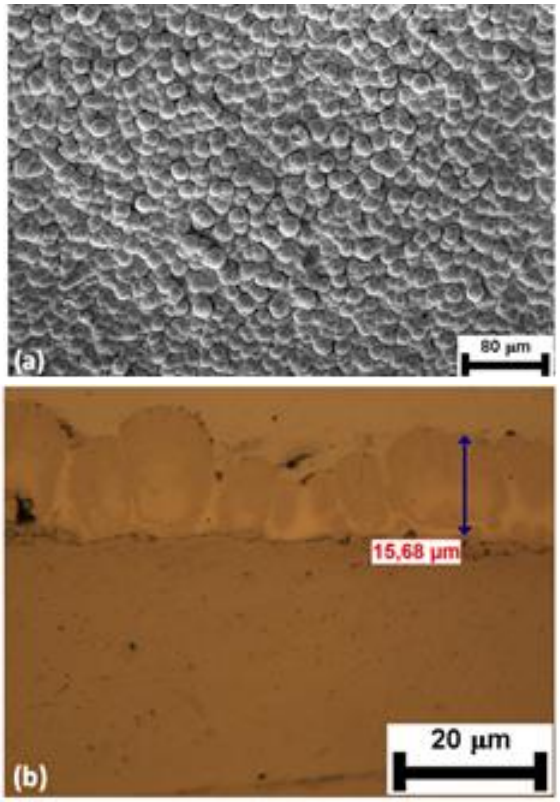

Fig. 1. (a) Morphological and (b) cross-sectional micrographs of the electroless Ni–B coating.

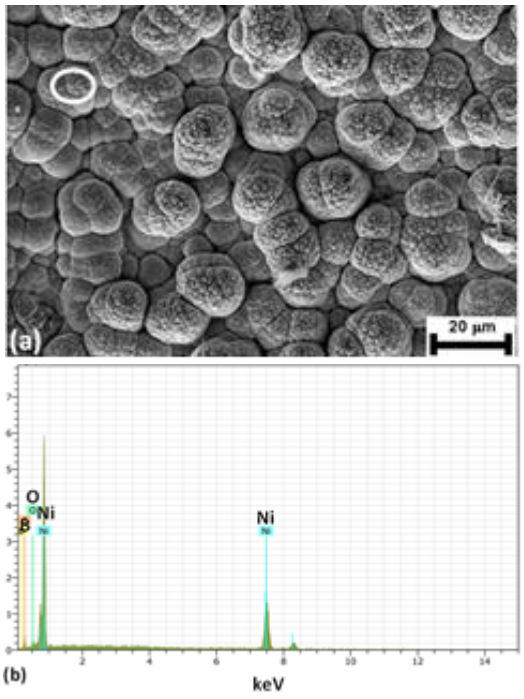

Fig. 2. EDS spectra and analysis results.

The XRD patterns of the untreated CP-Ti and Ni-B coated CP-Ti are given in Fig. 3. As expected, the untreated CP-Ti is entirely composed of hexagonal α-phase (denoted as "Ti" in Fig. 3). On the other hand, the XRD pattern in Fig. 3 indicates the formation of Ni–B deposit in amorphous phase on the surface of CP-Ti, which is observed with the development of a single broad peak around 45° which corresponding to Ni (111). The predominance of peak pertaining to amorphous phase with a corresponding absence in the intensity of the peaks pertaining to α-Ti confirms the formation of a thick (~15 μm) and homogeneous Ni-B layer (Fig. 1b), which would otherwise exhibit α-Ti as the predominant peak in the XRD pattern. In terms of Knoop microhardness, the formation of Ni-B film on the CP-Ti enables a significant improvement in cross-section hardness due to the presence of boron in the interstitial solid solution. Almost a three-fold increase in microhardness from 279 ±11 to 818 ±61 $HK_{0.01}$ is observed for CP-Ti after electroless Ni-B coating.

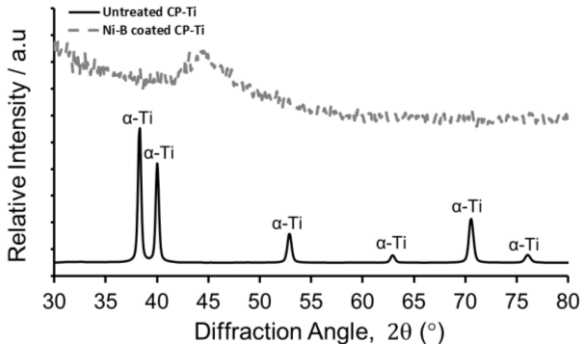

Fig. 3. XRD patterns of the untreated CP-Ti and Ni-B coated CP-Ti.

The tribocorrosion tests were performed at OCP conditions and the evolution of the potential as a function of time is shown in Fig. 4 along with their corresponding friction curves. The change in OCP of the untreated CP-Ti and Ni-B coated CP-Ti was measured before, during and after the sliding motion. Before sliding, the OCP of both untreated CP-Ti and Ni-B coated CP-Ti was about -320 mV. During the sliding, it can be clearly seen for the Ni-B coated CP-Ti that an initial drop in the OCP values at the beginning of the test was observed and then the Ni-B coated CP-Ti presented relatively stable OCP values. This indicates that the coating was not destroyed during sliding, hence no changes in the OCP until the end of the test. In fact, the cross-section scans performed across each wear showed that the wear scar depth for the Ni-B coated CP-Ti was 9 μm (Fig. 5). This clearly indicates that this coating was not fully penetrated. Therefore, the underlying CP-Ti substrate was neither exposed to the corrosive environment nor affected by plastic deformation. On the other hand, in case of the untreated CP-Ti, when sliding started, a sudden drop in the potential of ~630 mV can be observed. The voltage drop indicates the destruction of the passive layer at the contact region [24,25] suggesting an increase in susceptibility of the CP-Ti surface for corrosion, and therefore a need for surface protection. In this case, the wear scar depth of the untreated CP-Ti was found to be approximately 15 μm (Fig. 5). It should be noted that the OCP stayed low during the sliding, constant at about -950 mV, together with high oscillations that are usually attributed to the repeated action of depassivation and repassivation of the untreated CP-Ti under sliding against an Al2O3 ball [24,25]. Furthermore, the OCP during the wear test for the Ni-B coated CP-Ti was higher than the OCP of the untreated CP-Ti, indicating that the Ni-B coating was effective in protecting the untreated CP-Ti from corrosion during sliding. After the sliding motion was stopped, the untreated CP-Ti presented a shift in the noble direction with respect to the OCP, suggesting a progressive repassivation of the wear scar area, whereas the OCP values of the Ni-B coated CP-Ti became stable near the values recorded before the sliding started.

The untreated CP-Ti exhibited the highest and most unstable friction coefficient (Fig. 4 b), confirming its already known poor tribological characteristic, and thus the need for surface protective treatment. On the other hand, it can be clearly seen that the Ni-B coated CP-Ti showed a lower and more stable friction coefficient in comparison to the untreated CP-Ti substrate (Fig. 4 b). This could be attributed to the function of lubricant of the particles belonging to NiB coating with columnar structure under conditions of tribocorrosion (SAS solution). Accordingly, the Ni-B coated CP-Ti presented the low wear volume loss and the friction-reducing performance together with high amount of material transfer into the SAS solution (Table 2).

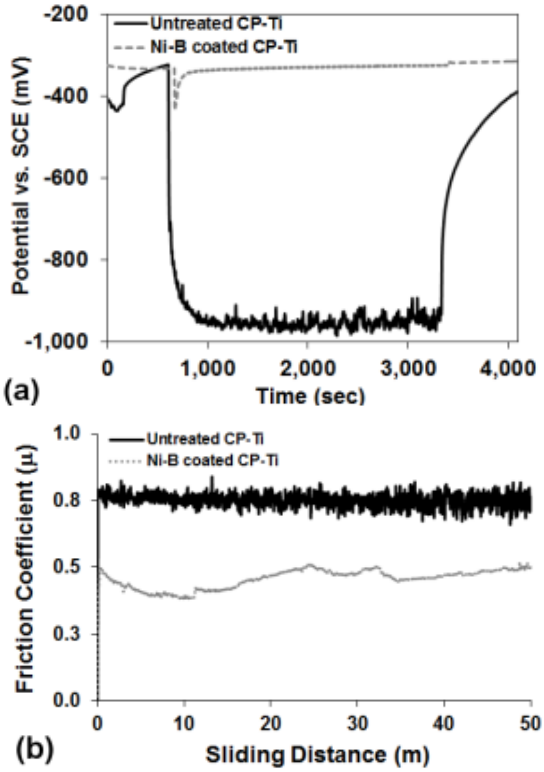

Fig. 4. The evolution of the (a) OCP and (b) friction coefficients recorded in-situ before, during and after sliding in SAS solution.

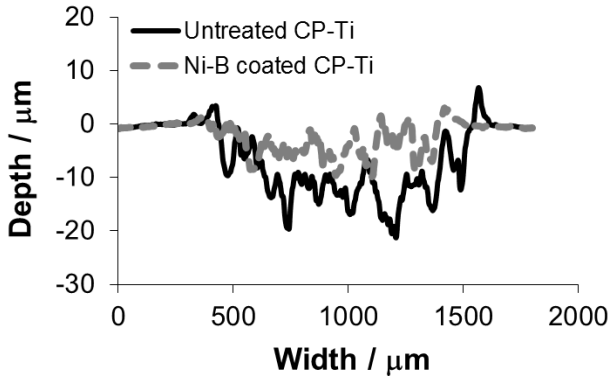

Fig. 5. Surface profiles across the wear scars of the untreated CP-Ti and Ni-B coated CP-Ti tested in SAS solution.

Table 2. Tribocorrosion test results of the untreated CP-Ti and the Ni-B coated CP-Ti.

Sample	Average friction coefficient	Wear volume loss (mm^3)	Optical density (a.u.)
Untreated CP-Ti	0.76	0.21	1.87
Ni-B coated CP-Ti	0.45	0.02	3.46

The low and high magnification views of the wear scars developed on the samples and their corresponding testing balls are shown in Fig. 6.

As can be seen in Fig. 6, the worn surface of the untreated CP-Ti exhibited obviously micro-cutting, plowing grooves and plastic deformation, and the worn surface of Ni-B coated CP-Ti was narrow with a smooth and polished appearance. It can be found that the size of worn surfaces of the Al_2O_3 balls is also similar to the results in Table 2.

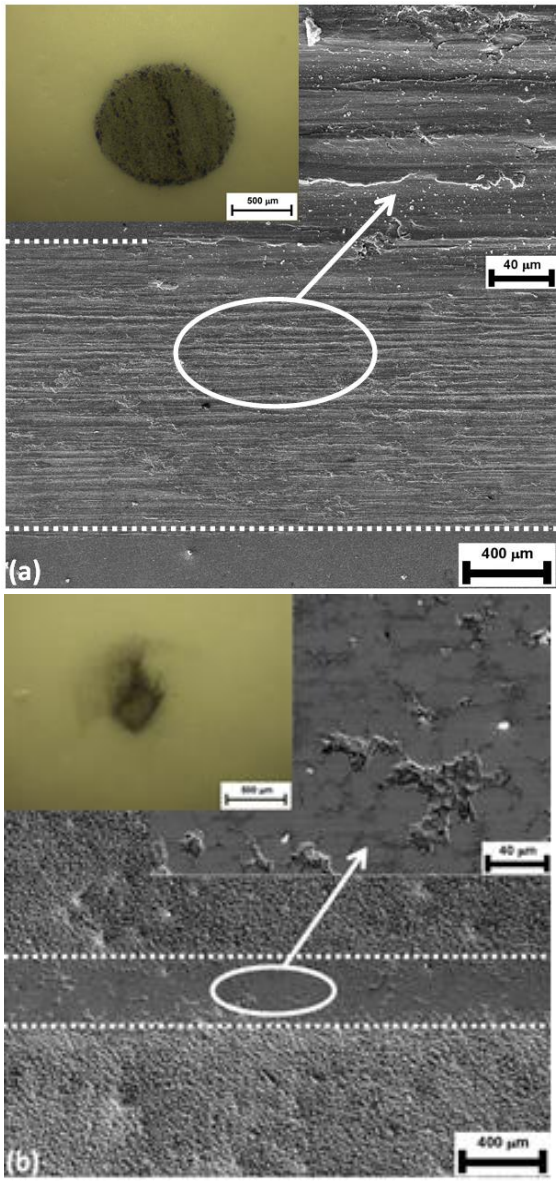

Fig. 6. Low and high magnification SEM micrographs of wear scars generated on the (a) untreated CP-Ti, (b) Ni-B coated CP-Ti, and LOM images of their corresponding testing balls after tribocorrosion.

Although the microhardness of the CP-Ti substrate was lower than that of Al_2O_3 ball, the CP-Ti had negative effects on the Al_2O_3 ball and the worn surface of the Al_2O_3 ball presented obvious plastic deformation, as shown in Fig. 6a because the amount of soft untreated CP-Ti

substrate transferred to the Al_2O_3 ball increased due to adhesion. Furthermore, the size of the worn surface of the Al_2O_3 ball in Fig. 6 b is significantly smaller than other, because of the existence of the self-lubricating Ni-B.

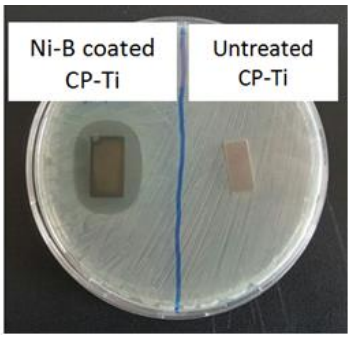

Fig. 7. The photograph of bacteria growth on culture plates after 24 h: the untreated CP-Ti and Ni-B coated CP-Ti samples.

Antibacterial activity of the untreated CP-Ti and the Ni-B coated CP-Ti on agar plate was examined on the diameter of basic inhibition zone of E. coli, gram-negative bacteria, using disc diffusion technique. A zone of bacterial growth inhibition with a dimension of 30 mm was seen for the Ni–B coated CP-Ti, while growth inhibition was not observed for the untreated CP-Ti used as a control for comparative analysis (Fig. 7). Thus, it appears that the Ni-B coated CP-Ti possess an excellent effectiveness in inhibition of bacterial growth comparing to the positive control. This could be attributed to the slight dissolving of Ni. It can be assumed that the release of Ni2+ from the Ni–B coating and its entry in bacterial cells can lead to a decrease of the bacterial growth. This mechanism has been proved for antibacterial activities of Ni–P coating [26].

4. CONCLUSIONS

A simple and cost-effective method was employed to modify the surface of commercial CP-Ti alloy. The results are summarized as follows:

- The surface modification on CP-Ti used as the substrate has been successfully carried out by electroless Ni–B deposition. XRD examination reveals that α-Ti phase for untreated CP-Ti and amorphous phase for Ni-B coated CP-Ti were obtained. The EDS analysis confirms the presence of Ni and B in the deposited layer. The LOM and SEM analyses show typical Ni–B coating structure with primary forms of a typical cauliflower-like morphology.
- Knoop microhardness of the modified surface reached 818 ±61 $HK_{0.01}$, which was extremely higher as compared with the hardness of the original CP-Ti substrate of 279 ±11 $HK_{0.01}$.
- Under OCP tribocorrosion conditions, the Ni-B coated CP-Ti exhibited better tribocorrosion performance when compared to the untreated CP-Ti. This was attributed to their improved frictional characteristics, and low wear scars depth that coincided with the absence of oscillations in the OCP.
- With an inhibition halo of 30 mm, the Ni–B coating exhibited a better biocidal effect on E. coli owing to less bacterial adhesion compared to the untreated CP-Ti control sample.

Acknowledgement

The authors wish to thank Gulcin CETIN from Biotechnology Application and Research Center (Bilecik, Turkey) for her help with the antibacterial experiments.

REFERENCES

[1] M. Kazemzadeh-Narbat, B.F.L. Lai, C. Ding, J.N. Kizhakkedathu, R.E.W. Hancock and R. Wang, 'Multilayered coating on titanium for controlled release of antimicrobial peptides for the prevention of implant-associated infections', *Biomaterials*, vol. 34, pp. 5969-5977, 2013.

[2] R. Caroline, 'Innovative surface treatments of titanium alloys for biomedical applications', *Materials Science Forum*, vol. 879, pp. 1570-1575, 2016.

[3] V.E. Annamalai, S. Kavitha and S.A. Ramji, 'Enhancing the properties of Ti6Al4V as a biomedical material: a review', *The Open Materials Science Journal*, vol. 8, pp. 1-17, 2014.

[4] A. Revathi, S. Magesh, V.K. Balla, M. Das and G. Manivasagam, 'Current advances in enhancement of wear and corrosion resistance of titanium alloys –a review', *Materials Technology: Advanced Performance Materials*, pp. 1-9, 2016.

[5] I.S.V. Marques, M.F. Alfaro, M.T. Saito, M.T. Saito, C. Takoudis, R. Landers, M.F. Mesquita, F.H.N. Junior, M.T. Mathew, C. Sukotjo and V.A.R. Baraok, 'Biomimetic coatings enhance tribocorrosion behavior and cell responses of commercially pure titanium surfaces', *Biointerphases*, vol. 11, no. 3, pp. 1-14, 2016.

[6] V. Totolin, V. Pejaković, T. Csanyi, O. Hekele, M. Huber and M.R. Ripoll, 'Surface engineering of Ti6Al4V surfaces for enhanced tribocorrosion performance in artificial seawater', *Materials and Design*, vol. 104, pp. 10-18, 2016.

[7] C. Richard, C. Kowandy, J. Landoulsi, M. Geetha and H. Ramasawmy, 'Corrosion and wear behavior of thermally sprayed nano ceramic coatings on commercially pure Titanium and Ti–13Nb–13Zr substrates', *Int. Journal of Refractory Metals & Hard Materials*, vol. 28, pp. 115–123, 2010.

[8] A. Zhecheva, W. Sha, S. Malinov and A. Long, 'Enhancing the microstructure and properties of titanium alloys through nitriding and other surface engineering methods', *Surface & Coatings Technology*, vol. 200, pp. 2192– 2207, 2005.

[9] H.D. Vora, R.S. Rajamure, S.N. Dahotre, Y.H. Ho, R. Banerjee and N.B. Dahotre, 'Integrated experimental and theoretical approach for corrosion and wear evaluation of laser surface nitrided, Ti–6Al–4V biomaterial in physiological solution', *Journal of The Mechanical Behavior of Biomedical Materials*, vol. 37, 153-164, 2015.

[10] H.G. Jeong, Y. Lee and D.G. Lee, 'Effects of pre-heat conditions on diffusion hardening of pure titanium by vacuum rapid nitriding', *Surface & Coatings Technology*, in Press, 2017.

[11] P. Stratton and M. Graf, 'Thermochemical surface treatment of titanium', *International Heat Treatment and Surface Engineering*, vol. 3, no. 1/2, pp. 26-29, 2009.

[12] K. Aniołek, M. Kupka and A. Barylski, 'Sliding wear resistance of oxide layers formed on a titanium surface during thermal oxidation', *Wear,* vol. 356-357, pp. 23–29, 2016.

[13] T. Hanawa, 'Biofunctionalization of titanium for dental implant', *Japanese Dental Science Review*, vol. 46, pp. 93—101, 2010.

[14] D. Teker, F. Muhaffel, M. Menekse, N.G. Karaguler, M. Baydogan and H. Cimenoglu, 'Characteristics of multi-layer coating formed on commercially pure titanium for biomedical applications', *Materials Science and Engineering C*, Vol. 48, pp. 579–585, 2015.

[15] H. Farnoush, F. Muhaffel and H. Cimenoglu, 'Fabrication and characterization of nano-HA–45S5 Bioglass composite coatings on calcium-phosphate containing micro-arc oxidized CP-Ti substrates', *Applied Surface Science*, vol. 324, pp. 765-774, 2015.

[16] M. Ipekci, F. Siyahjani and H. Cimenoglu, 'Thermochemical nitriding of commercial purity titanium', *Defect and Diffusion Forum*, vol. 334-335, pp. 117-121, 2013.

[17] S. Kikuchi and J. Takebe, 'Characterization of the surface deposition on anodized-hydrothermally treated commercially pure titanium after immersion in simulated body fluid', *Journal of Prosthodontic Research*, vol. 54, pp. 70–77, 2010.

[18] S. Ferraris, A. Venturello, M. Miola, A. Cochis, L. Rimondini and S. Spriano, 'Antibacterial and bioactive nanostructured titanium surfaces for bone integration', *Applied Surface Science*, vol. 311, pp. 279-291, 2014.

[19] F. Bulbul, 'Antibacterial activity of electroless Ni–B coating', *Materials Science and Technology*, vol. 27, no. 10, pp. 1540-1546, 2011.

[20] F. Mindivan and H. Mindivan, 'The study of electroless Ni-P/Ni-B duplex coating on HVOF-sprayed martensitic stainless steel coating', *Acta Physica Polonica A*, vol. 131, pp. 64-67, 2017.

[21] F. Delaunois and P. Lienard, 'Heat treatments for electroless nickel–boron plating on aluminium alloys', *Surface and Coatings Technology*, vol. 160 pp. 239–248, 2002.

[22] T. Watanabe and Y. Tanabe, 'The lattice images of amorphous-like Ni–B alloy films prepared by electroless plating method', *Transactions of the Japan Institute of Metals,* vol. 24, no. 6, pp. 396–404, 1983.

[23] V. Vitry, A.F. Kanta and F. Delaunois, 'Mechanical and wear characterization of electroless nickel-boron coatings', *Surface & Coatings Technology*, vol. 206, pp. 1879–1885, 2011.

[24] H. Mindivan, 'Comparative study of tribocorrosion properties of some bio-based materials in simulated artificial saliva', *Machines, Technologies, Materials*, vol. 12, pp. 58-60, 2016.

[25] F. Mindivan and H. Mindivan, 'Surface properties and tribocorrosion behaviour of a thermal sprayed martensitic stainless steel coating after pulsed plasma nitriding process', *Journal Advances in Materials and Processing Technologies*, vol. 2, no. 4, pp. 514-526, 2016.

[26] Z. Sharifalhoseini, M.H. Entezari and R. Jalal, 'Evaluation of antibacterial activity of anticorrosive electroless Ni–P coating against Escherichia coli and its enhancement by deposition of sono-synthesized ZnO nanoparticles', *Surface & Coatings Technology*, vol. 266, pp. 160–166, 2015.